Mathematical Biology and Bioinformatics
2022. V. 17. № S. P. t30–t41. doi: 10.17537/2022.17.t30

Ttranslation of the original article
Medvedev A.E. Mathematical Biology and Bioinformatics. 2022;17(2):312–324.
doi: 10.17537/2022.17.312

========== TRANSLATIONS OF PUBLISHED ARTICLES ==========

Construction of Complex Three-Dimensional Structures of the Aorta of a Particular Patient Using Finite Analytical Formulas

Medvedev A.E.

Khristianovich Institute of Theoretical and Applied Mechanics SB RAS, Novosibirsk, Russia
E. Meshalkin National Medical Research Center of the Ministry of Health of the Russian Federation, Novosibirsk, Russia

Abstract. A technique has been developed for constructing the geometry of a morphologically realistic human aorta, including the aortic root (Valsalva sinus), thoracic aorta, aortic arch with branches, and abdominal aorta with bifurcating vessels. The peculiarity of the technique is simple construction of an individual patient's aorta. The resulting three-dimensional model of the aorta is fully ready for 3D modeling and printing on a 3D printer.

Key words: *aorta, aortic arch, Valsalva sinus, mathematical modeling, aortic bifurcation, aneurism.*

INTRODUCTION

Modern clinical practice of curing cardio-vascular diseases is based on implanting minimally invasive hybrid prostheses and stent-grafts [1]. Increasing the efficiency of medical treatment requires permanent technological improvement of operation planning methods. For this purpose, doctors need a three-dimensional model of a vessel with individual pathological changes in patient's vessels. The final goal of the present study is the development of a method of rapid construction of an individual three-dimensional model of the human aorta on the basis of the key parameters of pathologies of a particular patient.

Currently available methods of construction a 3D model of the aorta (or its specific part) are based on processing MRT or CT images. A surgeon has to spent a long time on processing such images, and the result is often unsatisfactory. Moreover, because of a large number of unessential details, it is difficult to identify the main aorta pathologies. Aorta models based on MRT images require significant post-processing for 3D printing. Vascular surgeons often need some particular regions of the aorta and specific features of pathologies (aneurism size, etc.), while other regions are of minor importance.

The most frequent pathologies of the aorta are the aneurism (aorta expansion) and stenosis (aorta constriction). The death rate of patients with abdominal aneurism rupture is 65–85 % [2]. Various numerical methods are developed for modeling aorta pathologies [3]. Numerical modeling of the aorta aneurism usually starts from constructing a geometric model of the aorta. Simple symmetric [4] or asymmetric [5] models of the aneurism are often used. However, even for such geometrically simple models, researchers often provide only aneurism schemes without particular sizes and formulas used to construct the aneurism geometry. Numerical simulations of real aorta aneurism and stenosis are performed on the basis of 3D aorta models based on processing MRT or CT images of a particular patient [4, 6, 7]. It is next to impossible to retrieve the aorta geometry from these publications. A rare

exception is the paper [8], where the formulas and sizes for constructing a symmetric stenosis of the abdominal aorta are provided.

Iso-geometric construction of the complex geometry of the aorta can be performed using non-uniform rational B-splines (NURBS) [9, 10]. This method requires pre-processing of aorta visualization data. Then a vascular skeleton is extracted, and its segmentation into individual regions is performed; for these regions, a control grid (control points) and B-splines (based on these points) are generated. The segmented regions have to be matched with each other. As a result, a smooth model of the aorta in terms of B-splines is obtained. As was noted in [9], the NURBS model of the abdominal aorta requires aorta segmentation into 26 regions. The procedure consists of five steps (in addition to four steps of pre-processing of the results of patient's aorta visualization) of B-spline construction. The result is excellent, but requires a lot of manual processing of the model.

The proposed technique of constructing a 3D model is based on aorta segmentation into several regions with several parameters being specified for each region: type of the region (aorta bifurcation or single branch), input and output diameters, bending angle, and turning angle. An additional parameter for the aneurism or stenosis region is analytical definition of the pathology shape: length and overall size of the pathology and its angular size. The resultant method of the aorta (aorta region) is ready for 3D printing without additional post-processing. The model describes the specific features of the pathology of a particular patient and is fully ready for the pre-operation analysis.

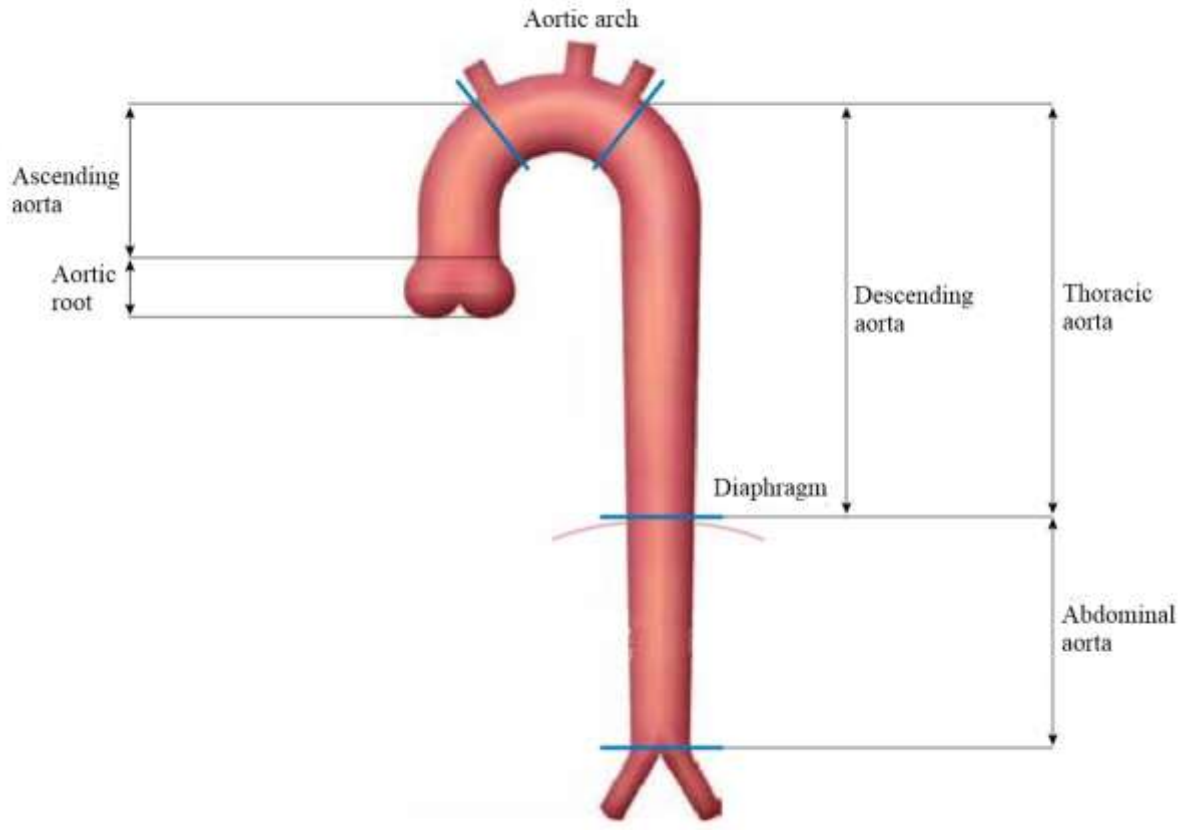

Fig. 1. Aorta segments.

AORTA SEGMENTS

The aorta is the main blood vessel through which blood flows from the left ventricle of the heart to the human organism. Approximately five liters of blood pass through the aorta in a minute (about 200 million liters of blood during the entire life time). The aorta segments are schematically shown in Figure 1. The aorta diameter of healthy patients is usually about

20 mm. The most frequent pathological changes in the aorta are the aneurism (expansion by more than 50 % of the normal diameter of the aorta) and thoracic aorta dissection.

The initial segment of the ascending aorta (aortic root) has three expansions – aorta (Valsalva) sinuses. Three arteries branch away from the aorta arch (subclavian and carotid arteries). The abdominal aorta is bifurcated at the end into two arteries.

CONTRUCTION OF THE VALSALVA SINUSES

The Valsalva sinuses were constructed in many studies as a procedure necessary for modeling aortic valve operation [11–19]. These researchers provided the characteristic sizes of the sinuses, geometry description, and algorithm for constructing the sinuses and entire aortic root. Unfortunately, there are no mathematical formulas used for the description of the 3D geometric model of the aortic root.

Construction of the Valsalva sinuses is based on the measurements of two projections of the aortic root [11] (Fig. 2).

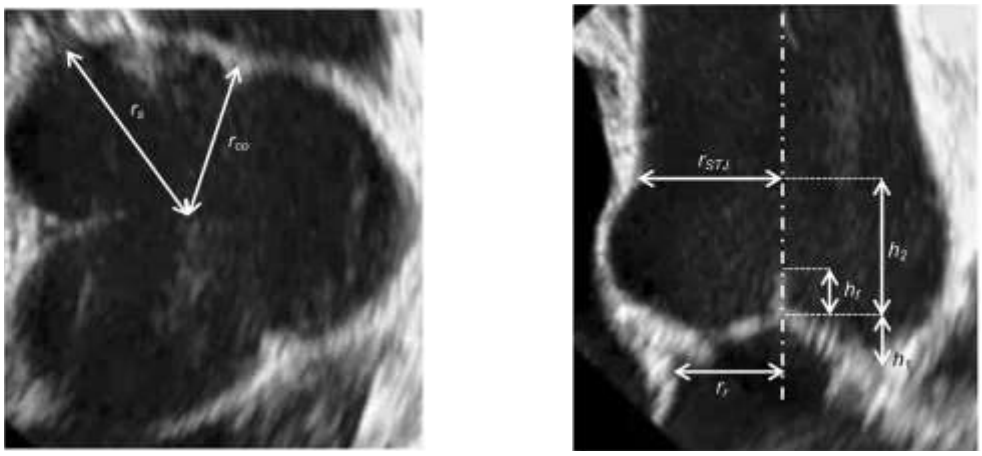

a) **b**)

Fig. 2. Measurements of the aortic root in the plane и $z = \text{const}$ (**a**) and in the plane $y = \text{const}$ (**b**) based on the result of 3D transesophageal echocardiography (3D-TEE) [11].

Construction of the Valsalva sinuses is based on the function

$$r_{0\_\sin}(\varphi;\alpha) = 0.5\left[1+\sin\left(\frac{\pi}{2}\frac{6\varphi-3\alpha-\pi}{\pi-3\alpha}\right)\right], \tag{1}$$

where φ is the angle, and the value of the parameter α is in the interval $0 \le \alpha < \frac{2}{3}\pi$. Using function (1), one can construct the cross section of the i-th $(i=1,2,3)$ Valsalva sinus in the plane $z = \text{const}$:

$$r_{i\_\sin}(\varphi;\alpha,i) = \begin{cases} 0, & \text{if } (i-1)\cdot\frac{2}{3}\pi \le \varphi < (i-1)\cdot\frac{2}{3}\pi+\alpha \\ r_{0\_\sin}\left(\varphi-(i-1)\cdot\frac{2}{3}\pi;\alpha\right), & \text{if } (i-1)\cdot\frac{2}{3}\pi+\alpha \le \varphi < i\cdot\frac{2}{3}\pi-\alpha \\ 0, & \text{if } i\cdot\frac{2}{3}\pi-\alpha \le \varphi < i\cdot\frac{2}{3}\pi \end{cases}. \tag{2}$$

Functions (1) and (2) are used to construct the cross section of the aortic root in the plane $z = \text{const}$, including all three Valsalva sinuses

$$r_{y\_\sin}(\varphi;\alpha)=\begin{cases} r_{i\_\sin}(\varphi;\alpha,1), \text{ if } 0\le\varphi<\dfrac{2}{3}\pi \\ r_{i\_\sin}(\varphi;\alpha,2), \text{ if } \dfrac{2}{3}\pi\le\varphi<\dfrac{4}{3}\pi \\ r_{i\_\sin}(\varphi;\alpha,3), \text{ if } \dfrac{4}{3}\pi\le\varphi<\dfrac{6}{3}\pi \end{cases}. \quad (3)$$

The cross section of the aortic root in the plane $z=\text{const}$ is defined by the functions

$$\begin{aligned} S_{x\_\sin}(\varphi;r_{co},r_s)&=\left[r_{co}+(r_s-r_{co})\,r_{y\_\sin}(\varphi;\alpha)\right]\cos(\varphi) \\ S_{y\_\sin}(\varphi;r_{co},r_s)&=\left[r_{co}+(r_s-r_{co})\,r_{y\_\sin}(\varphi;\alpha)\right]\sin(\varphi) \end{aligned}. \quad (4)$$

The cross section (4) is shown in Figure 3,a. The notation of the sizes in formulas (4) is consistent with that in Figure 2 from [11].

Construction of the cross section of the aortic root in the plane $y=\text{const}$ is based on the functions

$$z_{0\_\sin}(z;h_{1+2})=0.5\left[1+\sin\left(\frac{\pi}{2}\left(\frac{4z}{h_{1+2}}-1\right)\right)\right],\ z_l(z;h_{1+2},r_r,r_{STJ})=r_r+\frac{z}{h_{1+2}}(r_{STJ}-r_r), \quad (5)$$

where $h_{1+2}=h_1+h_2$. The cross section of the aortic root in the plane $y=\text{const}$ is defined by the function

$$z_{\sin}(z;h_{1+2},r_r,r_s,r_{STJ})=\pm\left\{z_l(z;h_{1+2},r_r,r_{STJ})+z_{0\_\sin}(z;h_{1+2})\cdot\left[r_s-z_l\left(\frac{h_{1+2}}{2};h_{1+2},r_r,r_{STJ}\right)\right]\right\}. \quad (6)$$

Function (6) is plotted in Figure 3,b.

The cross section functions (4) and (6) make it possible to construct a 3D model of the aortic root with the Valsalva sinuses as a two-parameter surface as a function of the variables (φ,z):

$$\begin{aligned} W_{\sin}(\varphi,z;\alpha,h_{1+2},r_r,r_s,r_{STJ})&=z_l(z;h_{1+2},r_r,r_{STJ})+ \\ &+r_{y\_\sin}(\varphi;\alpha)\cdot z_{0\_\sin}(z;h_{1+2})\cdot\left[r_s-z_l(z;h_{1+2},r_r,r_{STJ})\right]. \end{aligned} \quad (7)$$

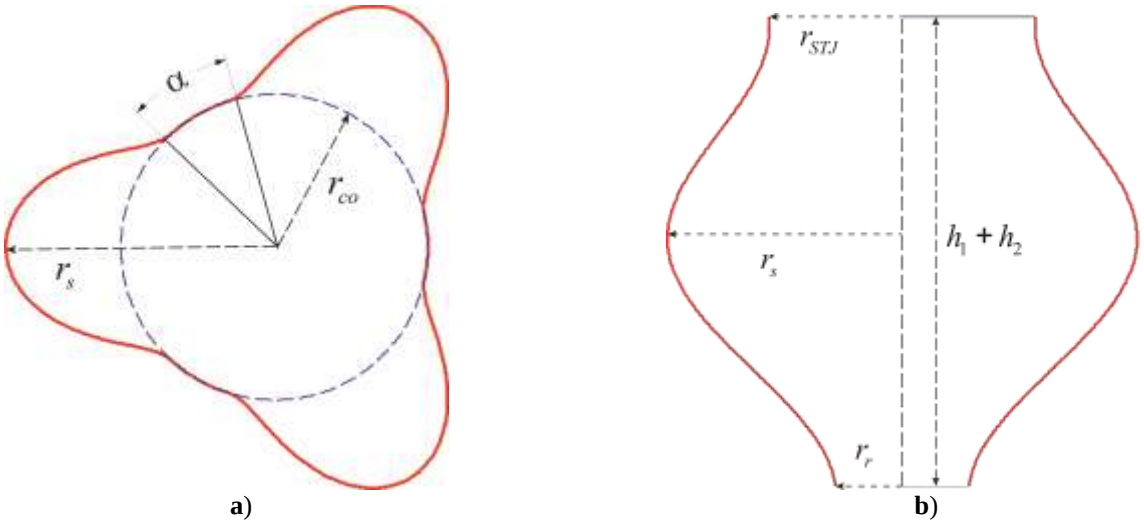

a) **b)**

Fig. 3. Cross sections of the aortic root in the plane $z=\text{const}$ (**a**) and in the plane $y=0$ (**b**).

The surface of the aortic root with the Valsalva sinuses in a 3D space (x, y, z) is defined by three functions

$$\begin{aligned} W_{x\_\sin}(\varphi, z; \alpha, h_{1+2}, r_r, r_s, r_{STJ}) &= W_{\sin}(\varphi, z; \alpha, h_{1+2}, r_r, r_s, r_{STJ}) \cdot \cos(\varphi), \\ W_{y\_\sin}(\varphi, z; \alpha, h_{1+2}, r_r, r_s, r_{STJ}) &= W_{\sin}(\varphi, z; \alpha, h_{1+2}, r_r, r_s, r_{STJ}) \cdot \sin(\varphi), \\ W_{z\_\sin}(z) &= z, \end{aligned} \tag{8}$$

where the variables φ and z change in the intervals $\varphi \in [0, 2\pi]$ and $z \in [0, h_{1+2}]$, respectively. The values of the parameters of the aortic root and Valsalva sinuses can be found in [11]: $r_r = 12$ mm, $r_s = 1.4 r_r$, $h_{1+2} = 1.4 r_r$, $r_{STL} = 1.1 r_r$, $r_{co} = 0.5(r_{STJ} + r_s)$, and $\alpha = 4^\circ$. The 3D model of the aortic root in the space (x, y, z) is shown in Figure 4.

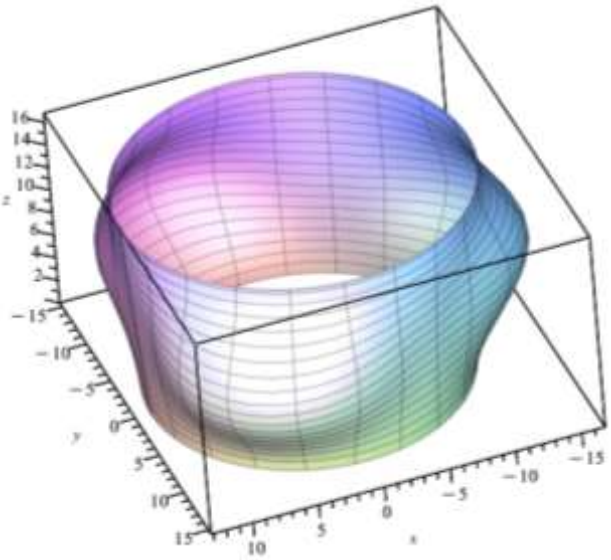

Fig. 4. Three-dimensional model of the aortic root.

CONSTRUCTION OF AORTA BRANCHES

There are three arteries branching almost at a right angle from the aorta arch (Fig. 1). Branching of these arteries can be modeled as intersections of two cylinders. Problems of this kind are often encountered in engineering applications. Knyazev and Ustinova [20] described parametric construction of the line of intersection of two cylinders. Let us derive formulas for constructing two intersecting cylinders. The scheme of intersection and the corresponding notations are given in Figure 5,a.

The equation of the intersection line of the cylinders (one-parameter curve in the space (x, y, z), which is the red curve in Figure 5,a) is

$$\begin{aligned} R_{x\_\text{cross}}(\varphi; R_b, Z_{\text{centr}}, \kappa) &= R_b \sqrt{1 - (\kappa \sin\varphi)^2} \\ R_{y\_\text{cross}}(\varphi; R_b, Z_{\text{centr}}, \kappa) &= R_b \kappa \sin\varphi \\ R_{z\_\text{cross}}(\varphi; R_b, Z_{\text{centr}}, \kappa) &= Z_{\text{centr}} - R_b \kappa \cos\varphi \end{aligned}, \tag{9}$$

where $Z_{\text{center}} = Z_{b\_\text{in}} + 0.5(Z_{b\_\text{out}} - Z_{b\_\text{in}})$ is the middle of the big cylinder along the z axis, and $\kappa = R_s / R_b$ is the ratio of the radii of the big and small cylinders.

Mathematical Biology and Bioinformatics. 2022. V. 17. № S. doi: 10.17537/2022.17.t30

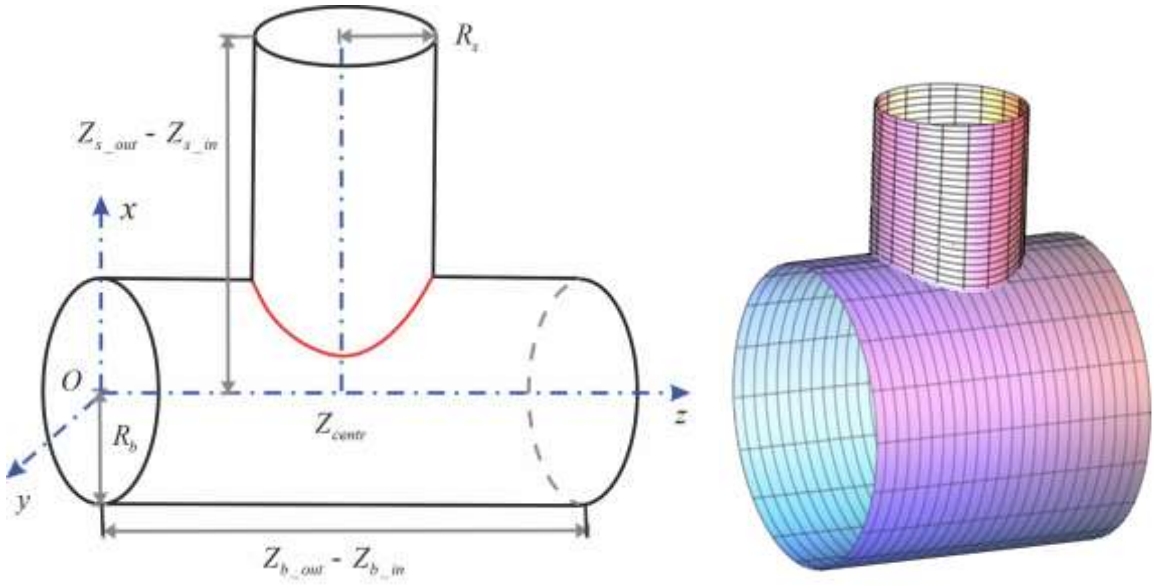

a) **b**)

Fig. 5. Intersection of two cylinders (**a**). The line of intersection of the cylinders is shown by the red curve (Eq. (9)). Three-dimensional model of intersection of the cylinders (**b**).

The intersecting cylinders are described by the following equations:

– big cylinder

$$\begin{aligned} C_{x\_b}(\varphi; R_b) &= R_b \cos\varphi \\ C_{y\_b}(\varphi; R_b) &= R_b \sin\varphi \\ C_{z\_b}(z) &= z \end{aligned}, \qquad (10)$$

where the angle is $\varphi \in [0, 2\pi]$, $z \in \left[z_{b\_\text{in}}, z_{b\_\text{out}} \right]$;

– small cylinder

$$\begin{aligned} C_{x\_s}(z) &= z \\ C_{y\_s}(\varphi; R_s) &= R_s \sin\varphi \\ C_{z\_s}(\varphi; R_s, Z_{\text{centr}}) &= Z_{\text{centr}} - R_s \cos\varphi \end{aligned}, \qquad (11)$$

where the angle is $\varphi \in [0, 2\pi]$, $z \in \left[R_{x\_\text{cross}}(\varphi; R_b, Z_{\text{centr}}, \kappa), Z_{s\_\text{out}} \right]$. The resultant 3D model of intersecting cylinders is shown in Figure 5,b.

AORTA ANEURISM AND STENOSIS

Frequent pathologies of the aorta are the aneurism (aorta expansion) and stenosis (aorta constriction). Let us derive analytical formulas for the description of local asymmetric constriction and expansion of the vessel.

Construction of vessel constriction and expansion is based on the functions

$$r_{0\_\text{an}}(s) = 0.5\left[1 + \sin\left(\frac{\pi}{2}(2s-1)\right)\right], \quad r_{\text{an}}(s) = \begin{cases} r_{0\_\text{an}}(2s), & \text{if } s \le 0.5 \\ r_{0\_\text{an}}(2(1-s)), & \text{if } s > 0.5 \end{cases}. \qquad (12)$$

The local unit function of deformation is defined by the function

$$R_{\text{an}}\left(s;s_{\text{beg}},s_{\text{end}}\right)=\begin{cases}0, & \text{if } s<s_{\text{beg}}\\ r_{\text{an}}\left(s\right), & \text{if } s_{\text{beg}}\le s<s_{\text{end}}\\ 0, & \text{if } s_{\text{end}}<s\end{cases}, \tag{13}$$

where s_{beg} and s_{end} are the points of deformation beginning and end $\left(s_{\text{beg}}<s_{\text{end}}\right)$.

The final function of constriction or expansion in terms of the vessel angle and length is the formula

$$F_{\text{an}}\left(\varphi,z;\varphi_{\text{beg}},\varphi_{\text{end}},z_{\text{beg}},z_{\text{end}},k_{\text{an}},H_{\text{an}}\right)=1+k_{\text{an}}H_{\text{an}}R_{\text{an}}\left(\varphi;\varphi_{\text{beg}},\varphi_{\text{end}}\right)R_{\text{an}}\left(z;z_{\text{beg}},z_{\text{end}}\right), \tag{14}$$

where φ_{beg} and φ_{end} are the angles of the beginning and end of vessel deformation $\left(0\le\varphi_{\text{beg}}<\varphi_{\text{end}}\le 2\pi\right)$, z_{beg} and z_{end} are the coordinates of deformation beginning and end along the vessel $\left(z_{\text{beg}}<z_{\text{end}}\right)$, k_{an} is the parameter of vessel expansion $\left(k_{\text{an}}=1\right)$ or constriction $\left(k_{\text{an}}=-1\right)$, and $H_{\text{an}}\ge 0$ is the magnitude of vessel deformation.

The equations for the cylinder with expansion or constriction have the form

$$\begin{aligned}A_x\left(\varphi,z;\varphi_{\text{beg}},\varphi_{\text{end}},z_{\text{beg}},z_{\text{end}},k_{\text{an}},H_{\text{an}}\right)&=C_x\left(\varphi;R\right)\cdot F_{\text{an}}\left(\varphi,z;\varphi_{\text{beg}},\varphi_{\text{end}},z_{\text{beg}},z_{\text{end}},k_{\text{an}},H_{\text{an}}\right),\\ A_y\left(\varphi,z;\varphi_{\text{beg}},\varphi_{\text{end}},z_{\text{beg}},z_{\text{end}},k_{\text{an}},H_{\text{an}}\right)&=C_y\left(\varphi;R\right)\cdot F_{\text{an}}\left(\varphi,z;\varphi_{\text{beg}},\varphi_{\text{end}},z_{\text{beg}},z_{\text{end}},k_{\text{an}},H_{\text{an}}\right),\\ A_z\left(z\right)&=C_z\left(\varphi;R\right),\end{aligned} \tag{15}$$

where R is the cylinder radius (10). Examples of the constructed aneurism and stenosis are shown in Figure 6.

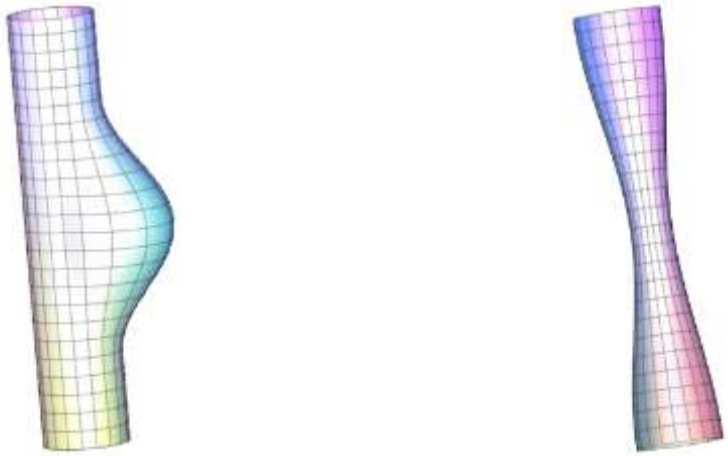

a) **b**)

Fig. 6. Examples of constructing 3D models of the vessel aneurism (**a**) and stenosis (**b**).

THREE-DIMENSIONAL MODEL OF THE AORTA

A technique of analytical construction of the human bronchial tree was developed in [21, 22]. This method can be extended to analytical construction of the human aorta.

An example of analytical construction of the thoracic aorta on the basis of the retrieved CT image of the aorta is shown in Figure 7. In reconstructing the CT image of the aorta (Fig. 7,a), there arise undesirable artifacts, which require further smoothing. This procedure is rather laborious and does not always provide a satisfactory result. For another patient (another CT image), the smoothing procedure has to be applied again.

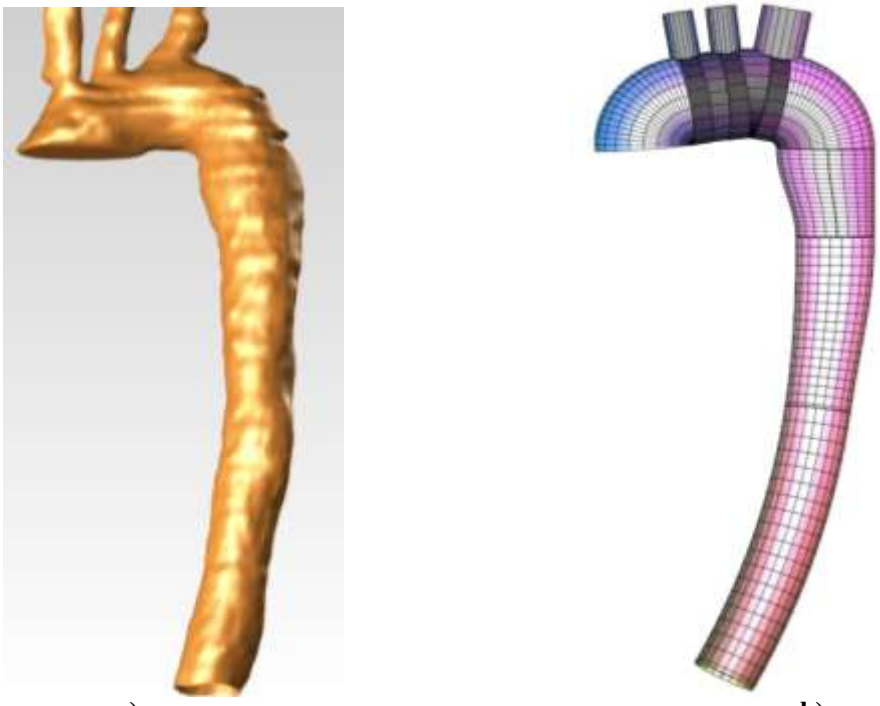

a) **b**)

Fig. 7. Construction of the thoracic aorta model. (**a**) Model of the thoracic aorta retrieved from patient's CT data. (**b**) Analytical model of the thoracic aorta.

In the proposed technique, the CT image of the aorta is divided into several basic segments (in the case presented here, into ten segments). Several parameters are specified for each segment:

1) segment number n;

2) segment type i: $i=0$ – aorta bifurcation (the formulas for constructing the vessel bifurcation can be found in [22]); $i=1$ – only the right branch of the bifurcation; $i=-1$ – only the left branch of the bifurcation; $i=2$ – cylindrical segment of the aorta (formula (10)); $i=3$ – aorta branching (formulas of intersecting cylinders (10), (11));

3) input radius of the aorta segment R_{in};

4) output radius of the aorta segment (right radius R_{out}^{+} and/or left radius R_{out}^{-}) – if the segment has only one output (no vessel bifurcation), then only one radius is specified, e.g., the right radius R_{out}^{+}; if there is a bifurcation, then the left output radius R_{out}^{-} of the bifurcation branch is also given);

5) output angle of the aorta segment(right angle χ_{out}^{+} and/or left angle χ_{out}^{-}) – if the segment has only one output (no vessel bifurcation), then only one angle is specified, e.g., the right angle χ_{out}^{+}; if there is a bifurcation, then the left output angle χ_{out}^{-} is also given);

6) angle σ_n of turning of the aorta segment around a local axis z (the formulas for the matrix of transformation of the local coordinate system can be found in [22]).

The parameters for analytical construction of the thoracic aorta are listed in Table 1. A specific feature of the constructed aorta model is smooth matching of the aorta segments (continuity of the derivative at the junction). The aorta model is ready for numerical simulation and 3D printing. The model is fully documented, and it can be reproduced by other researchers. To fit the model to another patient (another CT image of the aorta), it is necessary to change several parameters in the table of aorta segments. Thus, the process of aorta model design is significantly accelerated and simplified.

Table 1. Parameters for constructing the thoracic aorta model

n	i	L_{out}^{+}, mm	L_{out}^{-}, mm	R_{in}, mm	R_{out}^{+}, mm	R_{out}^{-}, mm	χ_n^{+}, deg	χ_n^{-}, deg	σ_n, deg	Segment type
0	1	170	–	15	15	–	85	–	0	Arch
1	3	–	–	15	–	4.5	–	–	0	Branching
2	1	6	–	15	15	–	3	–	0	Bending
3	3	–	–	15	–	4.5	–	–	0	Branching
4	1	6	–	15	15	–	17	–	0	Bending
5	3	–	–	15	–	7.5	–	–	0	Branching
6	1	100	–	15	15	–	80	–	0	Descending
7	1	30	–	15	12	–	1	–	135	Descending
8	1	60	–	12	10	–	10	–	10	Descending
9	1	100	–	10	10	–	20	–	100	Descending

Remark. The parameter $L_{\text{out}}^{\pm}$ is not the real length of the segment. The real length along the generatrix is proportional to the parameter $L_{\text{out}}^{\pm}$ and inversely proportional to the angle $\chi_n^{\pm}$. This dependence can be found in [22].

The aneurism and/or stenosis can be applied to any segment of the aorta. Figure 8 shows the application of the stenosis and aorta to the neighboring segments of the aorta.

Let us consider an example of abdominal aorta construction (Fig. 9). The parametric data for abdominal aorta construction are summarized in Table 2. Here segment 2 is an aorta bifurcation. Segments 3^{+} and 4^{+} represent the right branch of the bifurcation, and segments 3^{-} and 4^{-} represent the left branch of the bifurcation.

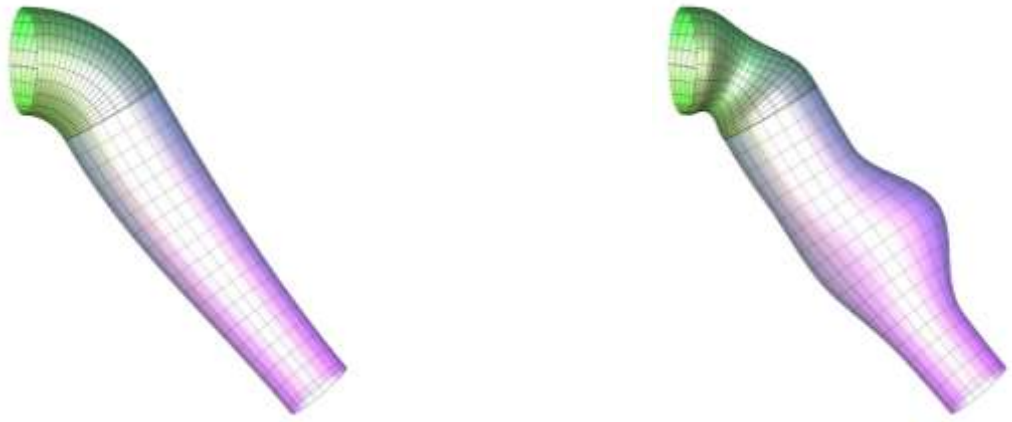

a) **b**)

Fig. 8. Examples of construction of the aneurism and stenosis of the thoracic aorta segment. (**a**) Healthy thoracic aorta. (**b**) Thoracic aorta with the stenosis and aneurism.

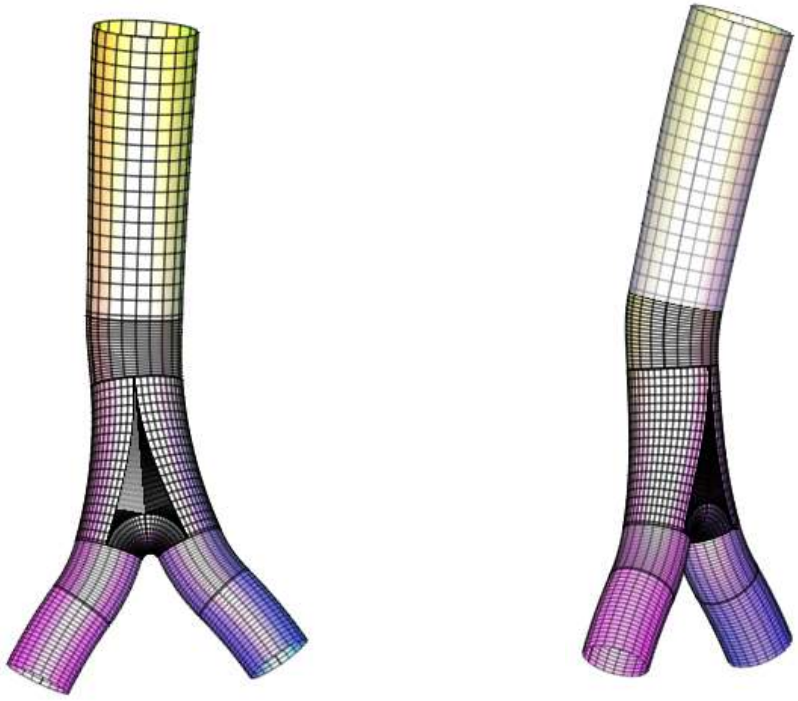

Fig. 9. Example of construction of the abdominal aorta segment.

Table 2. Parameter for constructing the abdominal aorta model

n	i	L_{out}^{+}, mm	L_{out}^{-}, mm	R_{in}, mm	R_{out}^{+}, mm	R_{out}^{-}, mm	χ_n^{+}, deg	χ_n^{-}, deg	σ_n, deg	Bifurcation type
0	1	50	–	9	8.15	–	5	–	90	Arch
1	1	11.8	–	8.15	7.775	–	15	–	0	Branching
2	0	31	–	7.775	5.84	5.84	20	20	–90	Bending
3^{+}	1	11	–	5.84	15	–	20	–	0	Branching
3^{-}	–1	–	11	5.84	15	–	–	20	0	Branching
4^{+}	1	15	–	5.84	15	–	–10	–	0	Bending
4^{-}	–1	–	15	5.84	15	–	–	–10	0	Bending

CONCLUSIONS

A technique has been developed for constructing the geometry of a morphologically realistic model of the human aorta, including the aortic root (Valsalva sinus), thoracic aorta, aortic arch with branches, and abdominal aorta with bifurcating vessels.

The development of a 3D model of the human aorta is required for planning surgical intervention and numerical modeling of the blood flow in the aorta. The anatomical structure of the aorta is different for different patients, especially if there are various pathologies (aneurism, stenosis, aorta dissection). Creation of an individual model of human aorta on the basis of MRT and CT images requires laborious manual work of a specialist with high computer skills.

A simple method of constructing a 3D model of the human aorta is proposed. Initially, a 3D model of the aorta (or particular aorta segment) of one patient is constructed. For this purpose, based on an unprocessed aorta model (an example of such an aorta is shown in

Figure 7,a), an analytical 3D model of this aorta is constructed (Fig. 7,b). For obtaining such an analytical aorta model, the aorta has to be divided into several segments, and the governing parameters for each segment have to be specified (Table 1). To construct an aorta model for another patient, the basic model is corrected with due allowance for individual specific features of the patient's aorta structure (his unprocessed aorta model). If necessary, pathological segments (stenosis and/or aneurism) are added. Correction of the basic model requires much less time and effort than creation of the model from scratch.

One of the key features of the technique is the simplicity of its application, which does not require monotonic manual labor aimed at constructing the individual patient's aorta. The resultant 3D aorta model is fully ready for 3D modeling and 3D printing. The aorta segments are matched with the second order of smoothness (continuous second derivative between the aorta segments).

The research was supported by RSF (project No. 22-15-20005).

REFERENCES

1. Chernyavskiy A.M., Lyashenko M.M., Tarkova A.R., Sirota D.A., Khvan D.S., Kretov E.I., Prokhorikhin A.A., Malaev D.U., Boykov A.A. Hybrid procedures for aortic arch disease. *Pirogov Journal of Surgery*. 2019. No. 4. P. 87–93. doi: 10.17116/hirurgia201904187
2. Sakalihasan N., Michel J-B., Katsargyris A., Kuivaniemi H., Defraigne J-O., Nchimi A., Powell J.T., Yoshimura K., Hultgren R. Abdominal aortic aneurysms. *Nature Reviews Disease Primers*. 2018. V. 4. No. 34. P. 1–22. doi: 10.1038/s41572-018-0030-7
3. Roy D., Kauffmann C., Delorme S., Lerouge S., Cloutier G., Soulez G. A literature review of the numerical analysis of abdominal aortic aneurysms treated with endovascular stent grafts. *Computational and Mathematical Methods in Medicine*. 2012. V. 2012. No. 820389. P. 1–16. doi: 10.1155/2012/820389
4. *Computational Modeling and Simulation Examples in Bioengineering*. 1st ed. Ed. Nenad Filipovic. Wiley, 2021. 384 p.
5. Scotti C.M., Shkolnik A.D., Muluk S.C., Finol E.A. Fluid-structure interaction in abdominal aortic aneurysms: effects of asymmetry and wall thickness. *BioMedical Engineering Online*. 2005. V. 4. No. 64. P. 1–22. doi: 10.1186/1475-925X-4-64
6. Skripachenko K.K., Golyadkina A.A., Morozov K.M., Chelnokova N.O., Ostrovsky N.V., Kirillova I.V., Kossovich L.Y. Biomechanical patient-oriented analysis of influence of the aneurysm on the hemodynamics of the thoracic aorta. *Russian Journal of Biomechanics*. 2019. V. 23. No. 4. P. 526–536. doi: 10.15593/RZhBiomeh/2019.4.03
7. Doyle B.J., Callanan A., McGloughlin T.M. A comparison of modelling techniques for computing wall stress in abdominal aortic aneurysms. *BioMedical Engineering Online*. 2007. V. 6. No. 38. P. 1–12. doi: 10.1186/1475-925X-6-38
8. Sinitsyna D.E., Yuhnev A.D., Zaytsev D.K., Turkina M.V. The flow structure in a three-dimensional model of abdominal aortic bifurcation: ultrasonic and numerical study. *St. Petersburg Polytechnical State University Journal. Physics and Mathematics*. 2019. V. 12. No. 4. P. 50–60. doi: 10.18721/JPM.12405
9. Zhang Y., Bazilevs Y., Goswami S., Bajaj C.L., Hughes T.J.R. Patient-Specific Vascular NURBS Modeling for Isogeometric Analysis of Blood Flow. *Computer Methods in Applied Mechanics and Engineering*. 2007. V. 196. No. 29–30. P. 2943–2959. doi: 10.1016/j.cma.2007.02.009
10. Coda M. *Advanced patient-specific modeling and analysis of complex aortic structures by means of Isogeometric Analysis*: PhD Dissertation. Pavia: University of Pavia, 2019. 172 p.

11. Rami Haj-Ali, Gil Marom, Zekry S.B., Rosenfeld M., Raanani E. A general three-dimensional parametric geometry of the native aortic valve and root for biomechanical modeling. *Journal of Biomechanics*. 2012. V. 45. No. 14. P. 2392–2397. doi: 10.1016/j.jbiomech.2012.07.017
12. De Hart J., Peters G.W.M., Schreurs P.J.G., Baaijens F.P.T. A three-dimensional computational analysis of fluid–structure interaction in the aortic valve. *Journal of Biomechanics*. 2003. V. 36. No. 1. P. 103–112. doi: 10.1016/S0021-9290(02)00244-0
13. Rankin J.S., Bone M.C., Fries P.M., Aicher D., Schäfers H-J., Crooke P.S. A refined hemispheric model of normal human aortic valve and root geometry. *Journal of Thoracic and Cardiovascular Surgery*. 2013. V. 146. No. 1. P. 103–108. doi: 10.1016/j.jtcvs.2012.06.043
14. Jatene M.B., Monteiro R., Guimarães M.H., Veronezi S.C., Koike M.K., Jatene F.B., Jatene A.D. Aortic Valve assessment. Anatomical study of 100 healthy human hearts. *Arquivos Brasileiros de Cardiologia*. 1999. V. 73. No. 1. P. 81–86. doi: 10.1590/S0066-782X1999000700007
15. Cao K., Bukac M., Sucosky P. Three-dimensional macro-scale assessment of regional and temporal wall shear stress characteristics on aortic valve leaflets. *Computer Methods in Biomechanics and Biomedical Engineering*. 2016. V. 19. No. 6. P. 603–613. doi: 10.1080/10255842.2015.1052419
16. Cao K., Sucosky P. Computational comparison of regional stress and deformation characteristics in tricuspid and bicuspid aortic valve leaflets. *International Journal for Numerical Methods in Biomedical Engineering*. 2017. V. 33. No. 3. P. 1–21. doi: 10.1002/cnm.2798
17. Wojciechowska D., Liberski A.R., Wilczek P., Butcher J., Scharfschwerdt M., Hijazi Z., Kasprzak J., Pibarot P., Bianco R. The optimal shape of an aortic heart valve replacement – on the road to the consensus. *QScience Connect*. 2017. V. 2017. No. 3. P. 1–14. doi: 10.5339/connect.2017.1
18. Thubrikar M. *The aortic valve*. Informa Healthcare: 2012. 232 p.
19. Redaelli A., Di Martino E., Gamba A., Procopio A.M., Fumero R. Assessment of the influence of the compliant aortic root on aortic valve mechanics by means of a geometrical model. *Medical Engineering and Physics*. 1997. V. 19. No. 8. P. 696–710. doi: 10.1016/S1350-4533(97)00033-7
20. Knyazev D.N., Ustinova E.S. Construction of the line of intersection of two cylinders in a parametric form. In: *Technical sciences in Russia and abroad*: Proc. IV Intern. Conf. (Moscow, January 2015). Moscow: Buki-Vedi, 2015. P. 122–125.
21. Medvedev A.E., Gafurova P.S. Analytical design of the human bronchial tree for healthy patients and patients with obstructive pulmonary diseases. *Mathematical Biology and Bioinformatics*. 2019. V. 14. No. 2. P. 635–648. doi: 10.17537/2019.14.635
22. Medvedev A.E. Method of Constructing an Asymmetric Human Bronchial Tree in Normal and Pathological Cases. *Mathematical Biology and Bioinformatics*. 2020. V. 15. No. 2. P. 148–157. doi: 10.17537/2020.15.148

Received 17.12.2022.
Published 26.12.2022.